NACA TN 2199 8623

TECH LIBRARY KAFB, NM
0065050

NATIONAL ADVISORY COMMITTEE FOR AERONAUTICS

TECHNICAL NOTE 2199

WIND-TUNNEL INVESTIGATION AT LOW SPEED OF THE LATERAL CONTROL CHARACTERISTICS OF AN UNSWEPT UNTAPERED SEMISPAN WING OF ASPECT RATIO 3.13 EQUIPPED WITH VARIOUS 25-PERCENT-CHORD PLAIN AILERONS

By Harold S. Johnson and John R. Hagerman

Langley Aeronautical Laboratory
Langley Air Force Base, Va.

Washington
October 1950

AFMDC
TECHNICAL LIBRARY
AFL 2811

TECH LIBRARY KAFB, NM

0065050

NATIONAL ADVISORY COMMITTEE FOR AERONAUTICS

TECHNICAL NOTE 2199

WIND-TUNNEL INVESTIGATION AT LOW SPEED OF THE LATERAL CONTROL CHARACTERISTICS OF AN UNSWEPT UNTAPERED SEMISPAN WING OF ASPECT RATIO 3.13 EQUIPPED WITH VARIOUS 25-PERCENT-CHORD PLAIN AILERONS

By Harold S. Johnson and John R. Hagerman

SUMMARY

A wind-tunnel investigation was made at low speed to determine the lateral control characteristics of an unswept untapered semispan wing of aspect ratio 3.13 equipped with 25-percent-chord plain unsealed ailerons having various spans and spanwise locations.

In general, changes in the wing angle of attack, aileron deflection, aileron span, and aileron spanwise location produced trends in the lateral control characteristics that were similar to but of different magnitude from those for unswept wings of higher aspect ratio. An aileron of a given percent span was most effective in producing roll when located outboard on the wing semispan, and this aileron also retained the greater part of its effectiveness through the angle-of-attack range in this spanwise position. The rate of change of hinge-moment coefficient with angle of attack C_{h_α} was relatively unaffected by aileron span and spanwise location. The rate of change of hinge-moment coefficient with aileron deflection C_{h_δ} became more negative as the span of outboard ailerons was increased and also as a half-span aileron was moved inboard on the semispan wing.

The results of this investigation indicated that existing empirical and theoretical relationships for predicting the aileron effectiveness parameter C_{l_δ} and the aileron hinge-moment parameters C_{h_α} and C_{h_δ} for various spans of ailerons gave satisfactory agreement with the experimental results.

INTRODUCTION

The National Advisory Committee for Aeronautics is making an extensive investigation of the lift and control effectiveness of various flaps and control surfaces on wings having plan forms suitable for transonic and supersonic airplanes. The objective is to obtain flap- and aileron-design criterions similar to those available for wings of conventional low-speed plan forms (reference 1 to 6). As part of this broad study, the lift and lateral control characteristics of an untapered low-aspect-ratio semispan wing having various amounts of sweep and equipped with 25-percent-chord plain unsealed flaps or ailerons having various spans and spanwise locations are being investigated in the Langley 300 MPH 7- by 10-foot tunnel.

This paper presents the results of the investigation of the unswept wing configuration having an aspect ratio of 3.13 and utilizing the 25-percent-chord control surfaces as ailerons. Rolling-moment, yawing-moment, and aileron-hinge-moment data were obtained through an aileron-deflection range from -30° to 30° at constant angles of attack ranging from -4° to about the angle of maximum lift. The results of investigations of the same semispan wing utilizing the 25-percent-chord control surfaces as lift flaps are presented in reference 7 for the model at 0° of sweep and in reference 8 for the model at 45° of sweepback.

SYMBOLS

The forces and moments measured on the wing are presented about the wind axes which, for the conditions of these tests (zero yaw), correspond to the stability axes. The lift, drag, pitching-moment, rolling-moment, and yawing-moment data are presented about the point shown in figure 1 which corresponds to the 25-percent-chord station of the mean aerodynamic chord.

The rolling-moment- and yawing-moment-coefficient data presented herein represent the aerodynamic effects on a complete wing produced by the deflection of the aileron on only the right semispan of the complete wing.

C_L lift coefficient (Twice lift of semispan model/qS)

C_D drag coefficient (Twice drag of semispan model/qS)

C_m pitching-moment coefficient (Twice pitching moment of semispan model/$qS\bar{c}$)

C_l rolling-moment coefficient (L/qSb)

C_n yawing-moment coefficient (N/qSb)

C_h aileron hinge-moment coefficient $\left(H/2qM_1\right)$

L rolling moment resulting from aileron deflection, foot-pounds

N yawing moment resulting from aileron deflection, foot-pounds

H aileron hinge moment, foot-pounds

M_1 area moment of aileron rearward of and about the hinge axis, feet^3 (see table I)

q free-stream dynamic pressure, pounds per square foot $\left(\frac{1}{2}\rho V^2\right)$

S twice area of semispan wing model, 19.16 square feet

b twice span of semispan model, 7.750 feet

$\bar{c}$ wing mean aerodynamic chord, 2.500 feet

c local wing chord, feet

y lateral distance from plane of symmetry, feet

b_a span of aileron, feet

V free-stream velocity, feet per second

ρ mass density of air, slugs per cubic foot

α angle of attack of wing with respect to chord plane at root of model, degrees

δ_a aileron deflection relative to wing-chord plane, measured perpendicular to aileron hinge axis (positive when trailing edge is down), degrees

α_δ control effectiveness parameter; that is, effective change in angle of attack caused by unit angular change in control-surface deflection

$$C_{l_\delta} = \left(\frac{\partial C_l}{\partial \delta_a}\right)_\alpha$$

$$C_{h_\alpha} = \left(\frac{\partial C_h}{\partial \alpha}\right)_{\delta_a}$$

$$C_{h_\delta} = \left(\frac{\partial C_h}{\partial \delta_a}\right)_\alpha$$

The subscripts outside the parentheses indicate the factor held constant. The parameters were measured at an angle of attack of 0° or an aileron deflection of 0°.

Subscripts:

a_i inboard end of aileron

a_o outboard end of aileron

CORRECTIONS

Jet-boundary corrections, determined by the method presented in reference 9, have been applied to the angle-of-attack and drag-coefficient values. Blockage corrections, to account for the constriction effects of the model and its wake, have also been applied to the test data (reference 10). The rolling-moment data were corrected for reflection-plane effects by the method of reference 11 by using unpublished experimental data for low-aspect-ratio wings. (See fig. 2.) No corrections have been applied to the data to account for the very small amount of wing twist produced by aileron deflection or for the small effect of air-flow leakage around the end plate at the root of the model.

MODEL AND APPARATUS

The semispan-wing model used in the investigation was constructed of laminated mahogany over a solid steel spar. The plan-form dimensions are shown in figure 1. The wing sections were NACA 64A010 and the model had 0° of sweepback, an aspect ratio of 3.13 (based on full-span dimensions), and a taper ratio of 1.0. The wing model had neither twist nor dihedral. A cross section of the wing showing the details of the 25-percent-chord unsealed plain ailerons is shown in figure 1. The ailerons were constructed of mahogany with steel spars and had joints at three spanwise stations so that various spans of ailerons at various spanwise locations could be investigated (fig. 1 and table I). When two or more aileron segments were tested in combination, the chordwise gaps between the aileron segments were sealed. A motor-driven aileron-actuating mechanism which was remotely controlled was used to obtain the various aileron deflections used in the investigation. The aileron deflections were constantly indicated on a meter by the use of a calibrated potentiometer that was mounted on the hinge axis near the root

chord of the model. The aileron hinge moments were measured by a calibrated electrical resistance type of strain gage.

The Langley 300 MPH 7- by 10-foot tunnel is a closed-throat, single-return tunnel. The semispan-wing model was mounted vertically in the tunnel with the root chord adjacent to the ceiling of the tunnel, which served as a reflection plane (fig. 3). The model was mounted on the six-component balance system so that all forces and moments acting on the model could be measured. A small clearance was maintained between the model and the tunnel ceiling so that no part of the model came into contact with the tunnel structure. A $\frac{1}{16}$-inch-thick metal end plate was attached to the root of the model to deflect the air flowing into the test section through the clearance hole in order to minimize the effect of this spanwise air flow on the flow over the model.

TESTS

All the tests were performed at an average dynamic pressure of approximately 100 pounds per square foot, which corresponds to a Mach number of 0.27 and a Reynolds number of about 4.5×10^6 based on the wing mean aerodynamic chord of 2.500 feet. Measurements have indicated that the tunnel turbulence factor is very close to unity.

Lateral-control tests with the various span ailerons were performed through an aileron-deflection range from -30° to 30° at constant angles of attack ranging from -4° to about 16° in approximately 4° increments.

RESULTS AND DISCUSSION

Wing Aerodynamic Characteristics

The lift, drag, and pitching-moment characteristics of the plain wing model are presented in figure 4. Since these data have been previously discussed in reference 7, where additional data for the wing with the various span control surfaces used as lift flaps have been presented, no detailed discussion is presented herein.

Aileron Control Characteristics

The variation of the aileron lateral control characteristics with aileron deflection is presented in figures 5 to 8 for the four spans of outboard ailerons $\left(y_{a_o} = 0.968\frac{b}{2}\right)$ and in figures 9 and 10 for the

approximately half-span ailerons $\left(b_a = 0.484\frac{b}{2}\right)$ at the inboard and midsemispan locations, respectively. A comparison of the experimental and estimated lateral-control parameters C_{l_δ}, C_{h_δ}, and C_{h_α} for the model equipped with outboard ailerons is presented in figure 11.

Rolling-moment characteristics.- The rolling-moment coefficients varied linearly with aileron deflection for deflections of less than about 20° and were relatively unaffected by angle-of-attack variations for values of α below approximately 12.6° (figs. 5 to 10). The data for the model with the control surfaces used as lift flaps (reference 7) show that the plain wing stalled at an angle of attack of about 16° and that positive deflections of the control surface decreased the angle of attack at which the wing stall occurs. At the highest angle of attack tested ($\alpha = 15.7°$) in the present investigation, the effects of wing stall are shown by the marked reduction in the rolling-moment coefficient for the larger positive aileron deflections; this effect became more pronounced as the aileron span was increased. For the angle-of-attack range investigated, only slight effects of α were noted for the negative aileron-deflection range. As expected, the rolling-moment coefficient increased as the span of the outboard aileron was increased (figs. 5 to 8). A study of the data for the half-span ailerons at three spanwise locations investigated (figs. 6, 9, and 10) reveals that the rolling-moment coefficient increased as the aileron was moved outboard and that the decrease in C_l with increase in α is smallest in relative magnitude for the half-span aileron at the outboard location. This ability of the outboard aileron to retain aileron effectiveness to higher angles of attack than the ailerons at the more inboard locations is thought to be caused by the initial stall that occurs on the inboard portion of the wing, whereas the outboard portion of the wing continues to load up and stalls at a higher angle of attack. (See references 7 and 12.)

As would be expected (reference 6), the experimental data for the model equipped with outboard ailerons (fig. 11 and table II) show that the aileron effectiveness parameter C_{l_δ} increased with increasing aileron span and that this variation of C_{l_δ} with aileron span is nonlinear. Estimated values of C_{l_δ} for the wing equipped with the midsemispan and inboard half-span ailerons, obtained from the experimental curve of figure 11 by taking the difference between the values of C_{l_δ} at the outboard and inboard ends of each aileron, are in excellent agreement with the results obtained for the wing equipped with the half-span ailerons at these two spanwise locations (table II). Because of this excellent agreement, the curve of figure 11 may be used to estimate the aileron effectiveness parameter of ailerons spanning various portions of the wing semispan on wings having plan forms similar to the wing

investigated. In agreement with data for other unswept wings of higher aspect ratio (for example, reference 13), these data indicate that an aileron of a given percent span is most effective when located outboard on the wing semispan.

The aileron effectiveness parameters for the various ailerons tested were computed by method I of reference 14. The value of the control effectiveness parameter α_δ used in these computations was 0.54 and was obtained from section data for the NACA 64A010 airfoil equipped with an unsealed flap type of control (reference 15), corrected for control chord by the method of reference 14. The agreement of the experimental and empirical values is very good (fig. 11); this agreement indicates that C_{l_δ} can be predicted satisfactorily by this method.

These variations of rolling moment with α, δ_a, aileron span, and aileron spanwise location are generally similar to but of different magnitude from those of other unswept wings of higher aspect ratios (references 4 to 6 and 14).

Yawing-moment characteristics.- The total yawing-moment coefficient resulting from equal up and down deflection of the ailerons was adverse (sign of yawing moment opposite to sign of rolling moment) throughout the angle-of-attack range investigated and was negligible at small angles of attack ($\pm 4^\circ$). The total yawing-moment coefficient became more adverse as the angle of attack was increased for all aileron configurations (figs. 5 to 10). The ratio of adverse yawing moments to total rolling moment increased as the angle of attack increased and was relatively unaffected by aileron span and spanwise location. For the higher aileron deflections $\left(\delta_a = 20^\circ \text{ to } 30^\circ\right)$ at $\alpha = 12.6^\circ$, these adverse yawing-moment coefficients were about 25 to 30 percent of the total rolling-moment coefficient. In the vicinity of the wing stall, the adverse yawing moments were much larger and might seriously reduce the rolling power of the ailerons; therefore, large rudder deflections would be required to perform a coordinated roll if the airplane directional stability were marginal. (See reference 16.)

Changes in angle of attack, aileron deflection, aileron span, and aileron spanwise location produced trends in the yawing-moment characteristics that were similar to those of unswept wings of higher aspect ratio (references 4 to 6 and 16).

Hinge-moment characteristics.- The hinge-moment parameter C_{h_α} was relatively unaffected by changes in aileron span or spanwise location (fig. 11 and table II). However, at large angles of attack, the variation of C_h with α was greatest for the outboard quarter-span aileron and decreased as the aileron span increased (figs. 5 to 8). These larger hinge-moment variations for the short-span outboard ailerons result from

a region of high loading located at the trailing edge of the wing near the tip at large effective angles of attack (references 7 and 12). The hinge-moment parameter C_{h_δ} became more negative as the span of the outboard ailerons $\left(y_{a_o} = 0.968\frac{b}{2}\right)$ was increased and also as the half-span aileron was moved inboard (fig. 11 and table II). The variation of C_h with δ_a was relatively unaffected by changes in angle of attack.

A comparison of the estimated hinge-moment parameters C_{h_δ} and C_{h_α}, computed for the various aileron spans by the method of reference 17, and the experimental values is also shown in figure 11. The estimated and experimental values are in good agreement, except possibly for the C_{h_α} values for short-span outboard ailerons.

Changes in α, δ_a, b_a, and aileron spanwise location produced trends in the hinge-moment characteristics that were similar to those of higher-aspect-ratio unswept wings (references 6, 13, and 17).

CONCLUSIONS

A wind-tunnel investigation was made at low speed to determine the lateral control characteristics of an unswept untapered semispan wing of aspect ratio 3.13 equipped with 25-percent-chord unsealed plain ailerons having various spans and spanwise locations. The results of the investigation led to the following conclusions:

1. Changes in the wing angle of attack, aileron deflection, aileron span, and spanwise location generally produced trends in the lateral control characteristics that were similar to but of different magnitude from those of unswept wings of higher aspect ratios.

2. An aileron of a given percent span would be most effective when located outboard on the wing semispan and this aileron would also retain the greater part of its effectiveness through the angle-of-attack range in this spanwise position.

3. The rate of change of hinge-moment coefficient with angle of attack C_{h_α} was relatively unaffected by aileron span and spanwise location. The rate of change of hinge-moment coefficient with aileron deflection C_{h_δ} became more negative as the span of outboard ailerons was increased and also as a half-span aileron was moved inboard on the semispan wing.

4. The aileron effectiveness parameter C_{l_δ} and the hinge-moment parameters C_{h_δ} and C_{h_α} for various spans of ailerons can be satisfactorily predicted by existing empirical and theoretical methods.

Langley Aeronautical Laboratory
National Advisory Committee for Aeronautics
Langley Air Force Base, Va., June 15, 1950

REFERENCES

1. House, R. O.: The Effects of Partial-Span Plain Flaps on the Aerodynamic Characteristics of a Rectangular and a Tapered Clark Y Wing. NACA TN 663, 1938.

2. House, Rufus O.: The Effects of Partial-Span Slotted Flaps on the Aerodynamic Characteristics of a Rectangular and a Tapered N.A.C.A. 23012 Wing. NACA TN 719, 1939.

3. Wenzinger, Carl J.: The Effects of Full-Span and Partial-Span Split Flaps on the Aerodynamic Characteristics of a Tapered Wing. NACA TN 505, 1934.

4. Weick, Fred E., and Jones, Robert T.: Résumé and Analysis of N.A.C.A. Lateral Control Research. NACA Rep. 605, 1937.

5. Pearson, Henry A., and Jones, Robert T.: Theoretical Stability and Control Characteristics of Wings with Various Amounts of Taper and Twist. NACA Rep. 635, 1938.

6. Langley Research Staff (Compiled by Thomas A. Toll): Summary of Lateral-Control Research. NACA Rep. 868, 1947.

7. Johnson, Harold S., and Hagerman, John R.: Wind-Tunnel Investigation at Low Speed of an Unswept Untapered Semispan Wing of Aspect Ratio 3.13 Equipped with Various 25-Percent-Chord Plain Flaps. NACA TN 2080, 1950.

8. Johnson, Harold S., and Hagerman, John R.: Wind-Tunnel Investigation at Low Speed of a 45° Sweptback Untapered Semispan Wing of Aspect Ratio 1.59 Equipped with Various 25-Percent-Chord Plain Flaps. NACA TN 2169, 1950.

9. Polhamus, Edward C.: Jet-Boundary-Induced-Upwash Velocities for Swept Reflection-Plane Models Mounted Vertically in 7- by 10-Foot, Closed, Rectangular Wind Tunnels. NACA TN 1752, 1948.

10. Herriot, John G.: Blockage Corrections for Three-Dimensional-Flow Closed-Throat Wind Tunnels, with Consideration of the Effect of Compressibility. NACA RM A7B28, 1947.

11. Swanson, Robert S., and Toll, Thomas A.: Jet-Boundary Corrections for Reflection-Plane Models in Rectangular Wind Tunnels. NACA Rep. 770, 1943.

12. Norton, F. H., and Bacon, D. L.: Pressure Distribution over Thick Aerofoils – Model Tests. NACA Rep. 150, 1922.

13. Schneiter, Leslie E., and Naeseth, Rodger L.: Wind-Tunnel Investigation at Low Speed of the Lateral Control Characteristics of Ailerons Having Three Spans and Three Trailing-Edge Angles on a Semispan Wing Model. NACA TN 1738, 1948.

14. Lowry, John G., and Schneiter, Leslie, E.: Estimation of Effectiveness of Flap-Type Controls on Sweptback Wings. NACA TN 1674, 1948.

15. Dods, Jules B., Jr.: Wind-Tunnel Investigation of Horizontal Tails. IV – Unswept Plan Form of Aspect Ratio 2 and a Two-Dimensional Model. NACA RM A8J21, 1948.

16. Fehlner, Leo F.: A Study of the Effect of Adverse Yawing Moment on Lateral Maneuverability at a High Lift Coefficient. NACA ARR, Sept. 1942.

17. Toll, Thomas A., and Schneiter, Leslie E.: Approximate Relations for Hinge-Moment Parameters of Control Surfaces on Swept Wings at Low Mach Numbers. NACA TN 1711, 1948.

TABLE I

DIMENSIONAL CHARACTERISTICS OF THE VARIOUS 0.25c AILERONS TESTED ON AN UNSWEPT SEMISPAN WING OF ASPECT RATIO 3.13

Configuration	Aileron span, $\frac{b_a}{b/2}$	Aileron spanwise location		M_1 (ft^3)
		$\frac{y_{a_i}}{b/2}$	$\frac{y_{a_o}}{b/2}$	
	0.968	0	0.968	0.7324
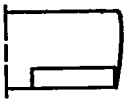	.726	.242	.968	.5493
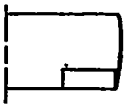	.484	.484	.968	.3662
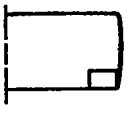	.242	.726	.968	.1831
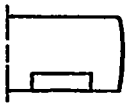	.484	.242	.726	.3662
	.484	0	.484	.3662

TABLE II

SUMMARY OF THE LATERAL-CONTROL PARAMETERS OF 0.25c AILERONS OF VARIOUS SPANS AND SPANWISE LOCATIONS ON AN UNSWEPT SEMISPAN WING OF ASPECT RATIO 3.13

Aileron span, $\frac{b_a}{b/2}$	C_{l_δ}	C_{h_δ}	C_{h_α}
0.968	0.00262	-0.0093	-0.0014
.726	.00238	-.0083	-.0012
.484	.00178	-.0067	-.0010
.242	.00093	-.0052	-.0011
[a].484	.00144	-.0073	-.0011
[b].484	.00073	-.0084	-.0015

[a]Midsemispan location
[b]Inboard location

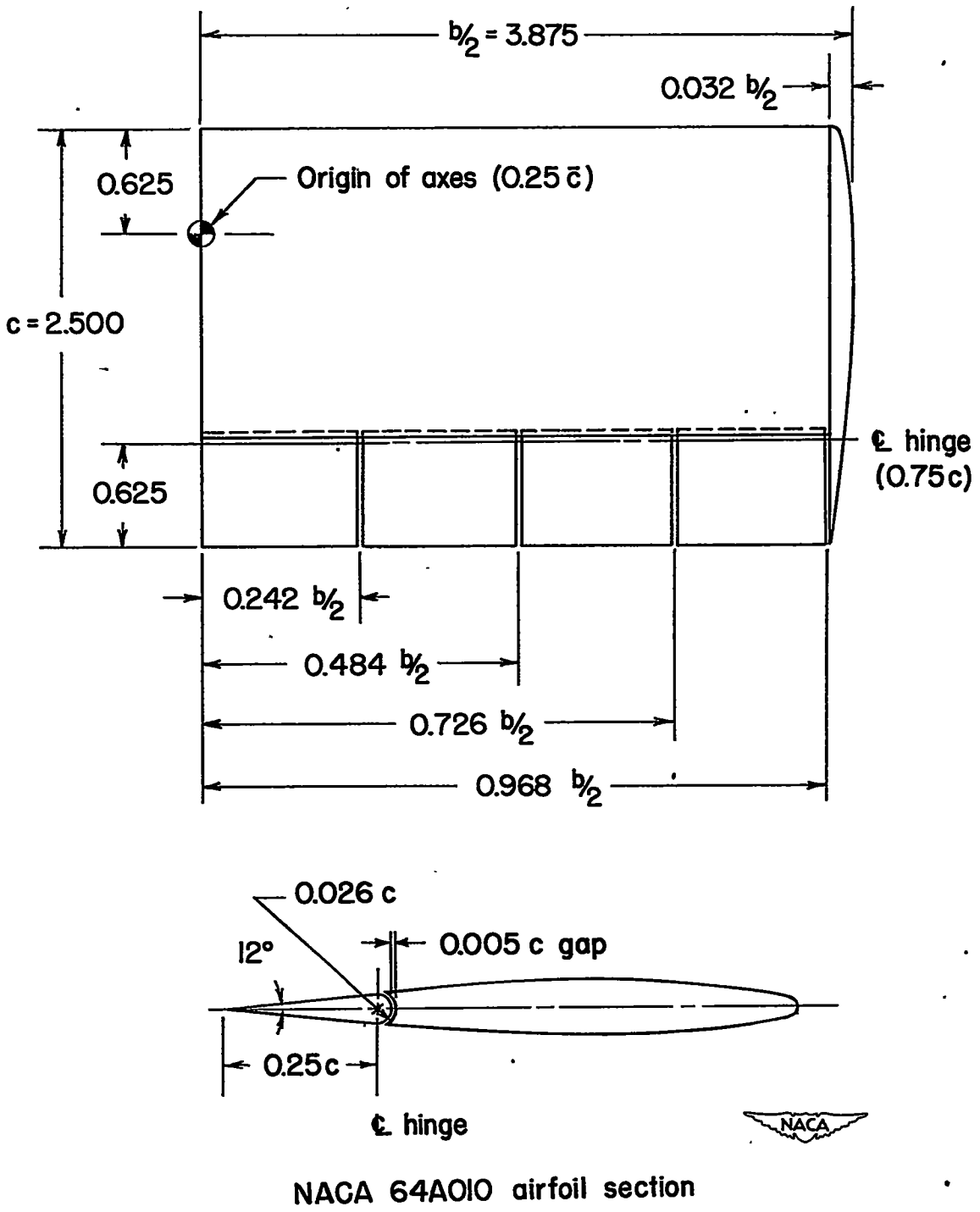

Figure 1.- Drawing of the unswept semispan wing having an aspect ratio of 3.13. (All dimensions are in feet.)

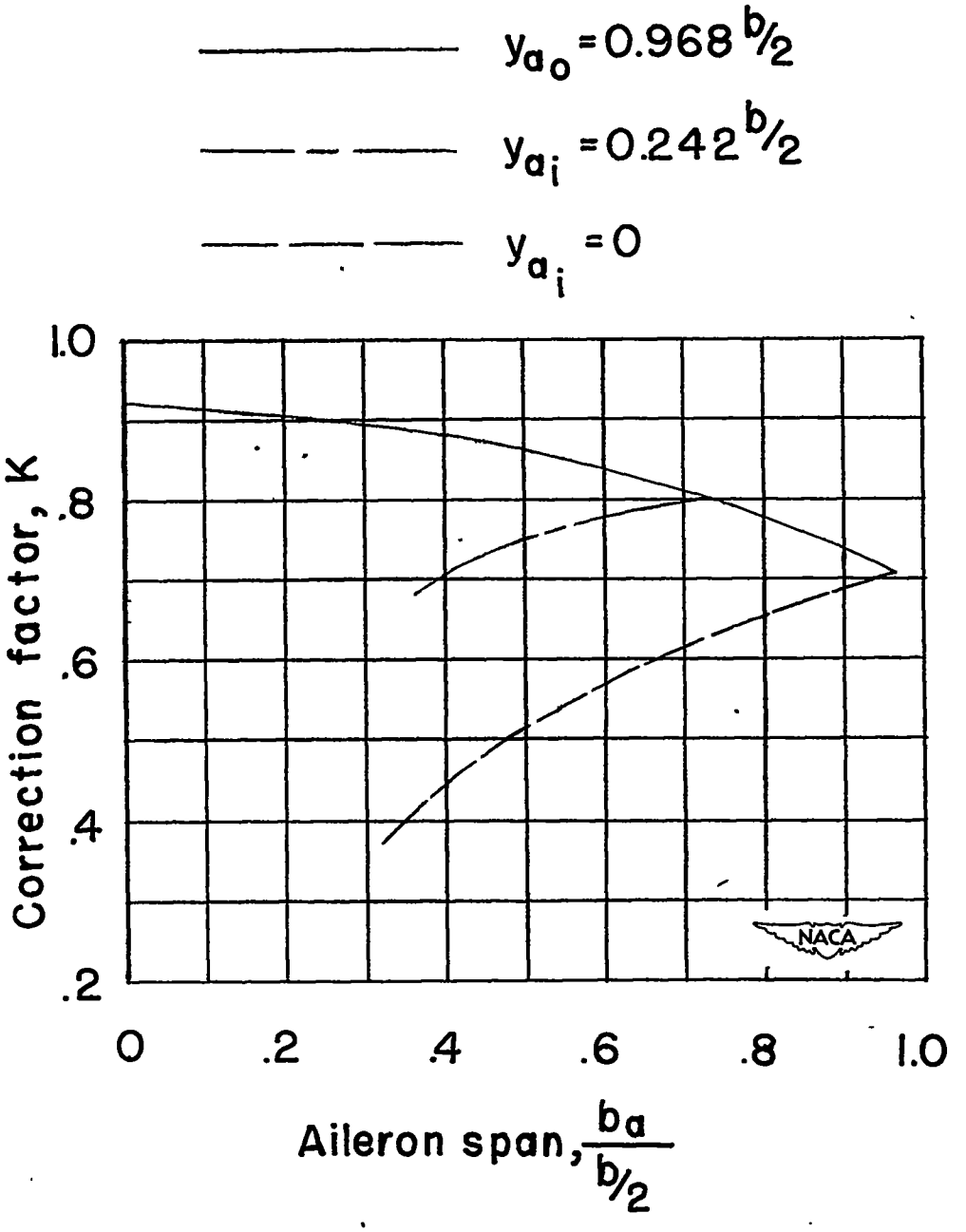

Figure 2.- Reflection-plane correction factor for rolling-moment coefficients. $\left(C_l = KC_{l_{Measured}}\right)$

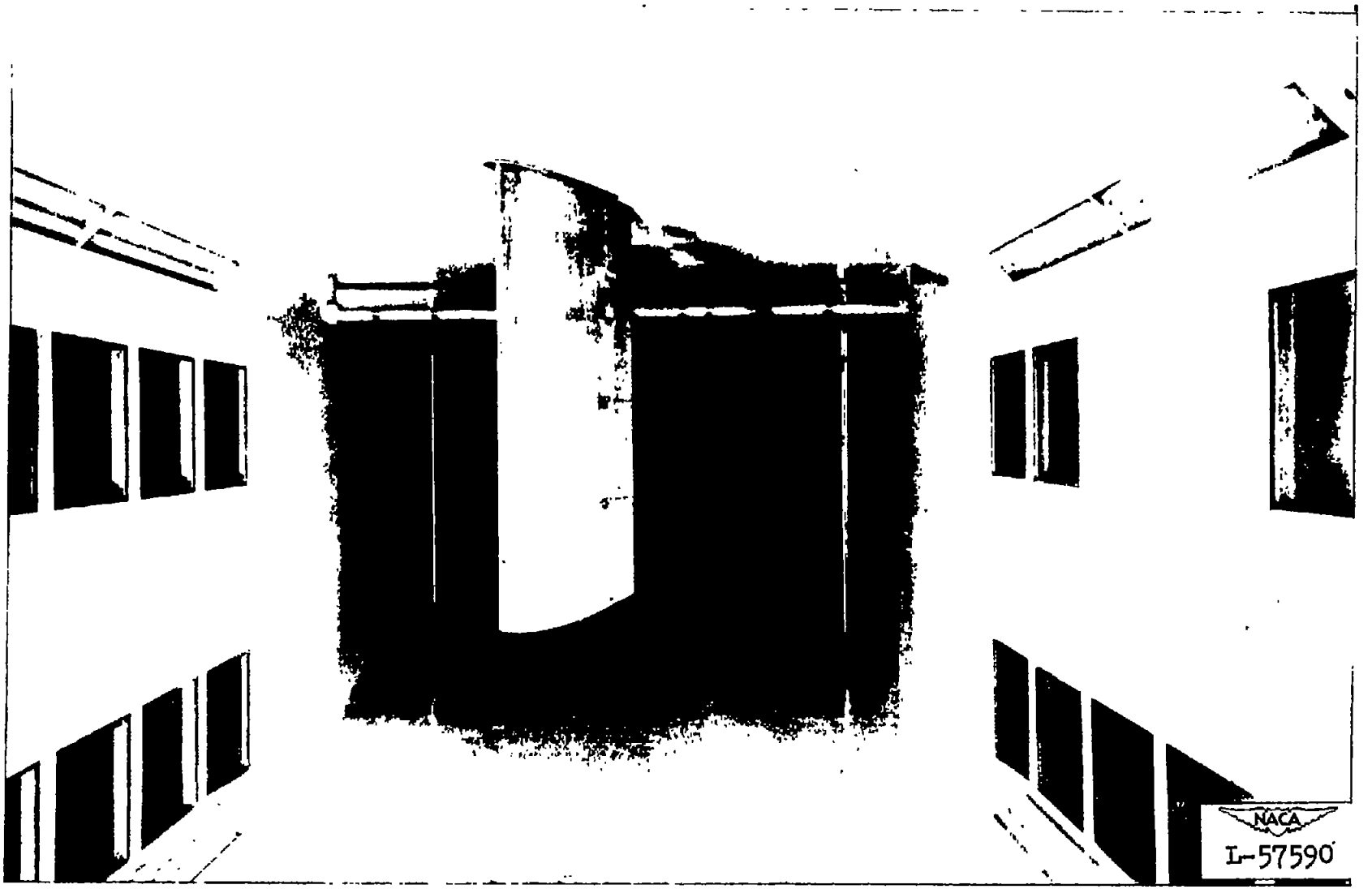

Figure 3.- Photograph of the unswept semispan wing having an aspect ratio of 3.13 mounted in the Langley 300 MPH 7- by 10-foot tunnel.

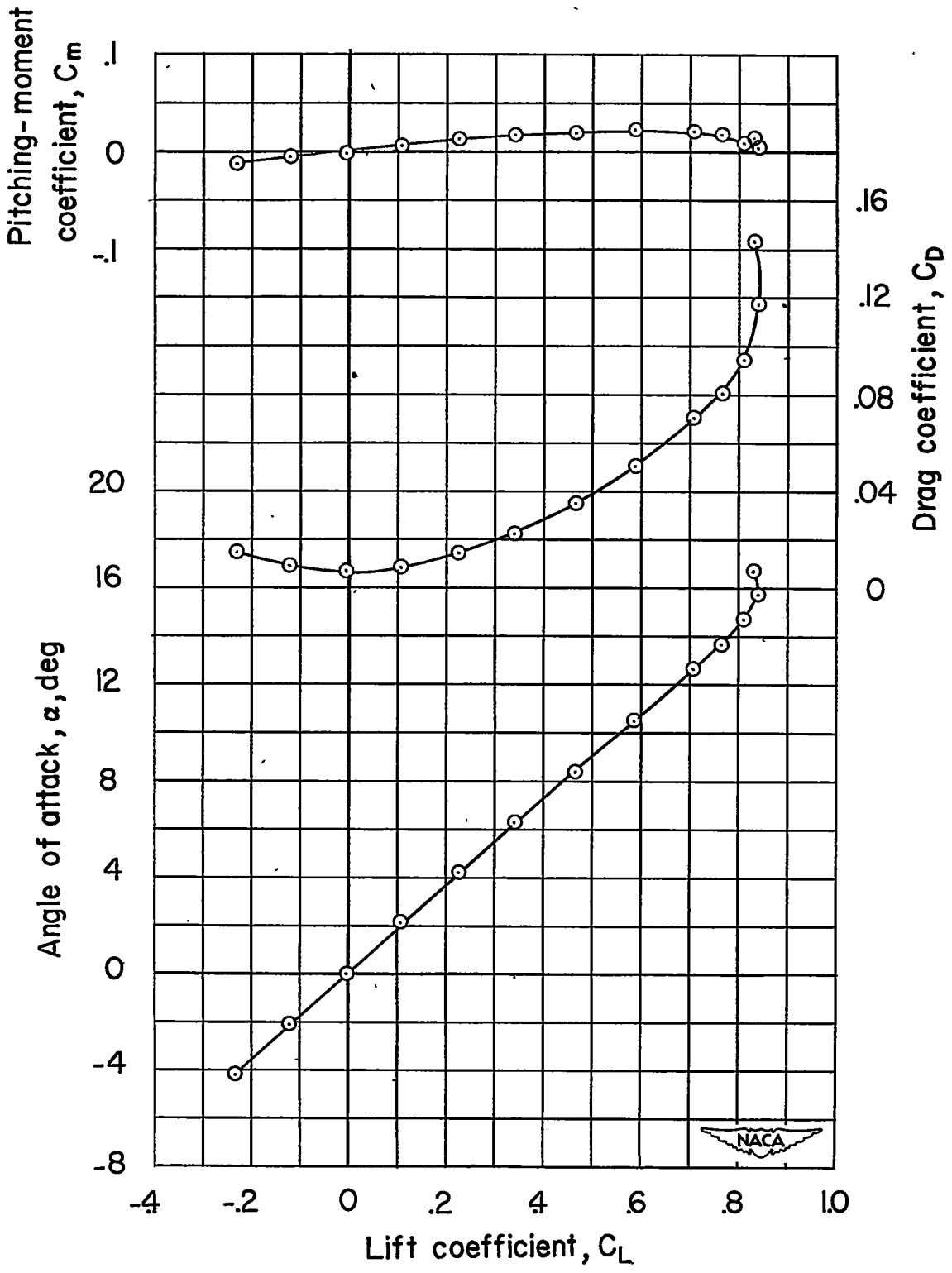

Figure 4.- Aerodynamic characteristics in pitch of the plain unswept semispan wing having an aspect ratio of 3.13.

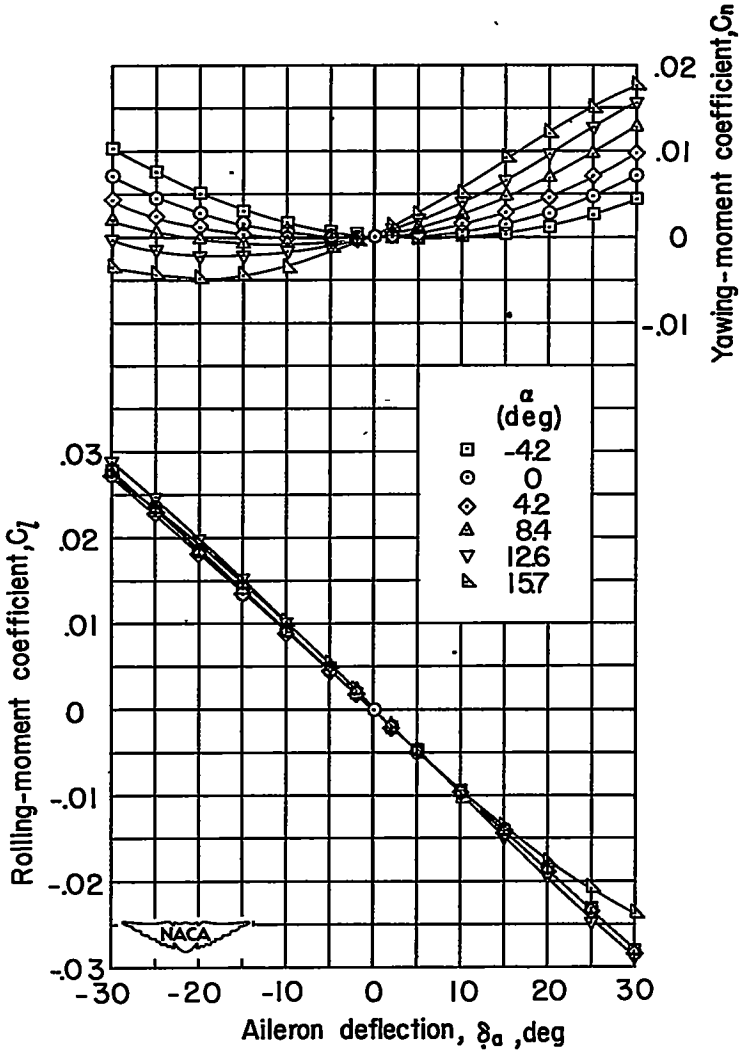

Figure 5.- Variation of lateral control characteristics with aileron deflection on the unswept semispan wing having an aspect ratio of 3.13. $b_a = 0.242\frac{b}{2}$; $y_{a_i} = 0.726\frac{b}{2}$; $y_{a_o} = 0.968\frac{b}{2}$.

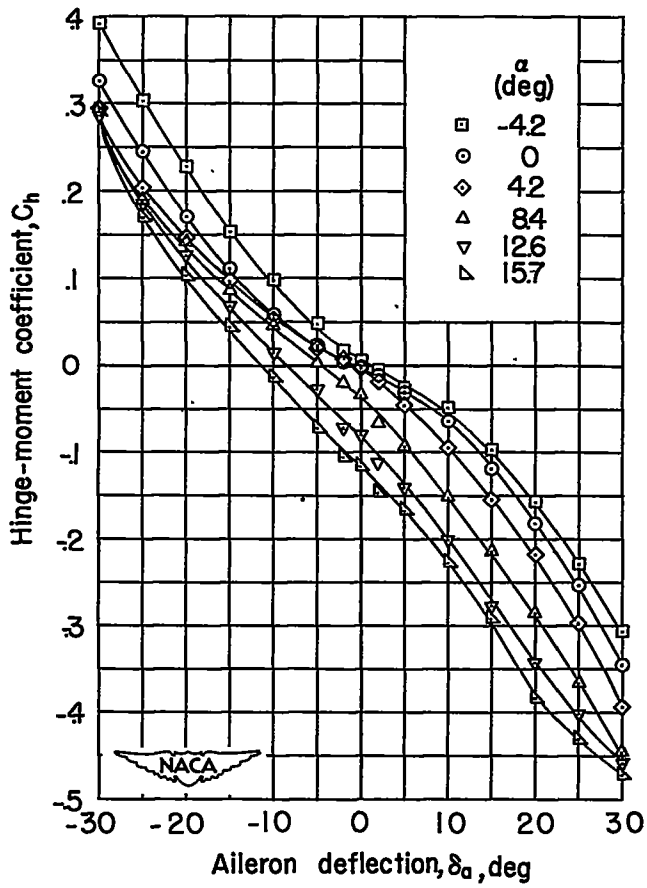

Figure 5.- Concluded.

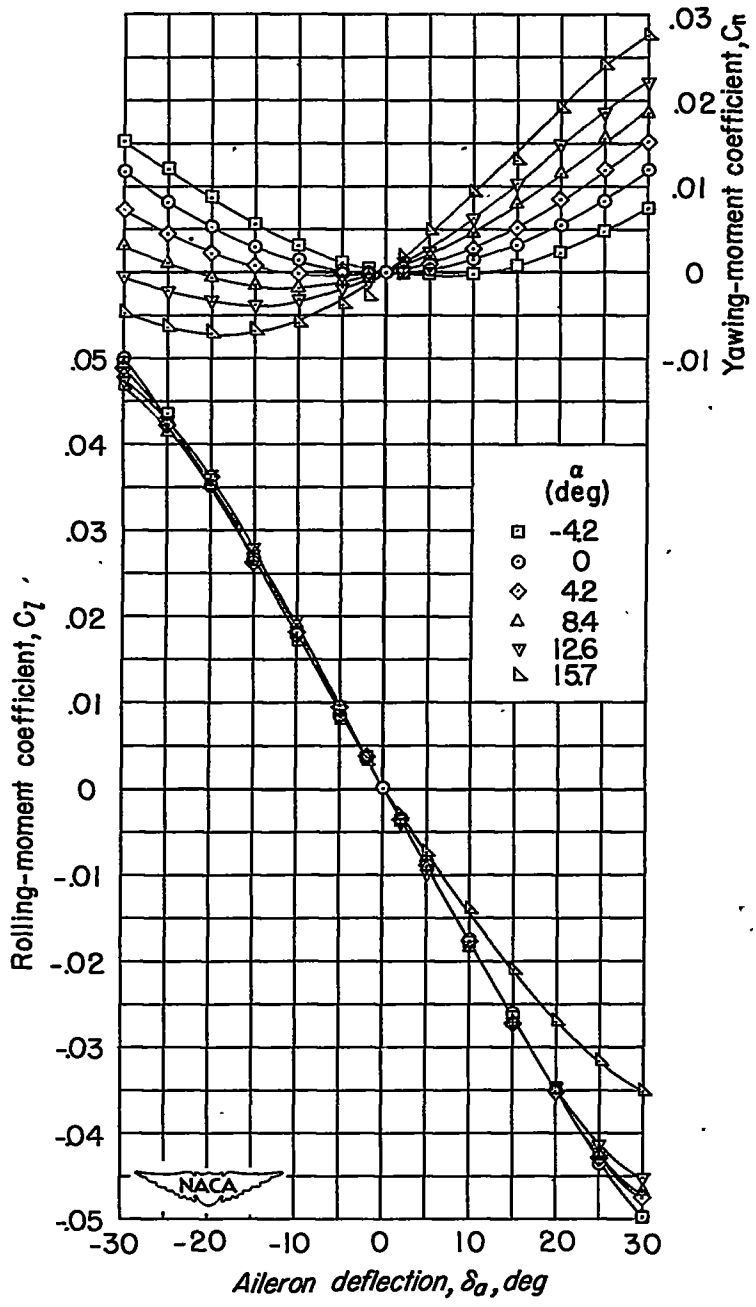

Figure 6.- Variation of lateral control characteristics with aileron deflection on the unswept semispan wing having an aspect ratio of 3.13. $b_a = 0.484\frac{b}{2}$; $y_{a_i} = 0.484\frac{b}{2}$; $y_{a_o} = 0.968\frac{b}{2}$.

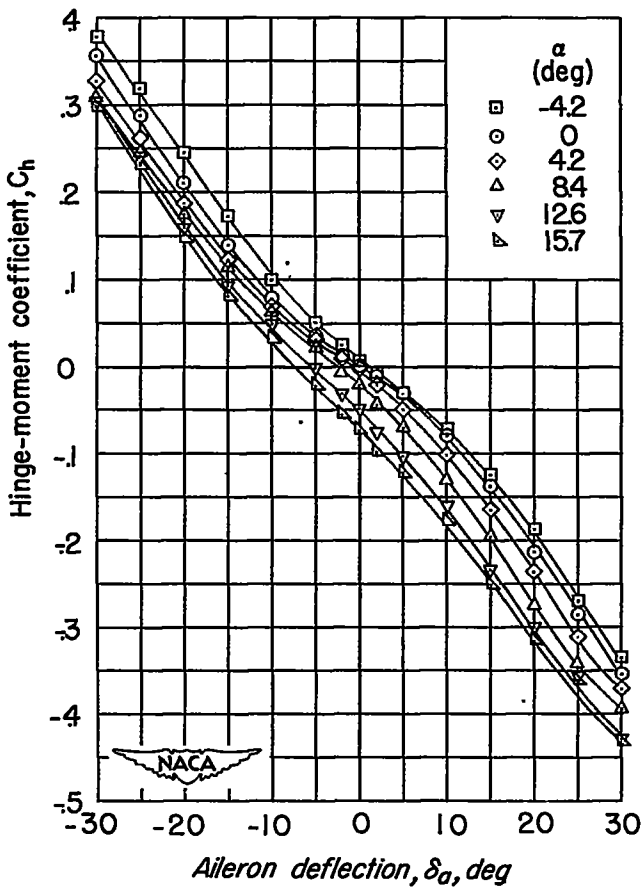

Figure 6.- Concluded.

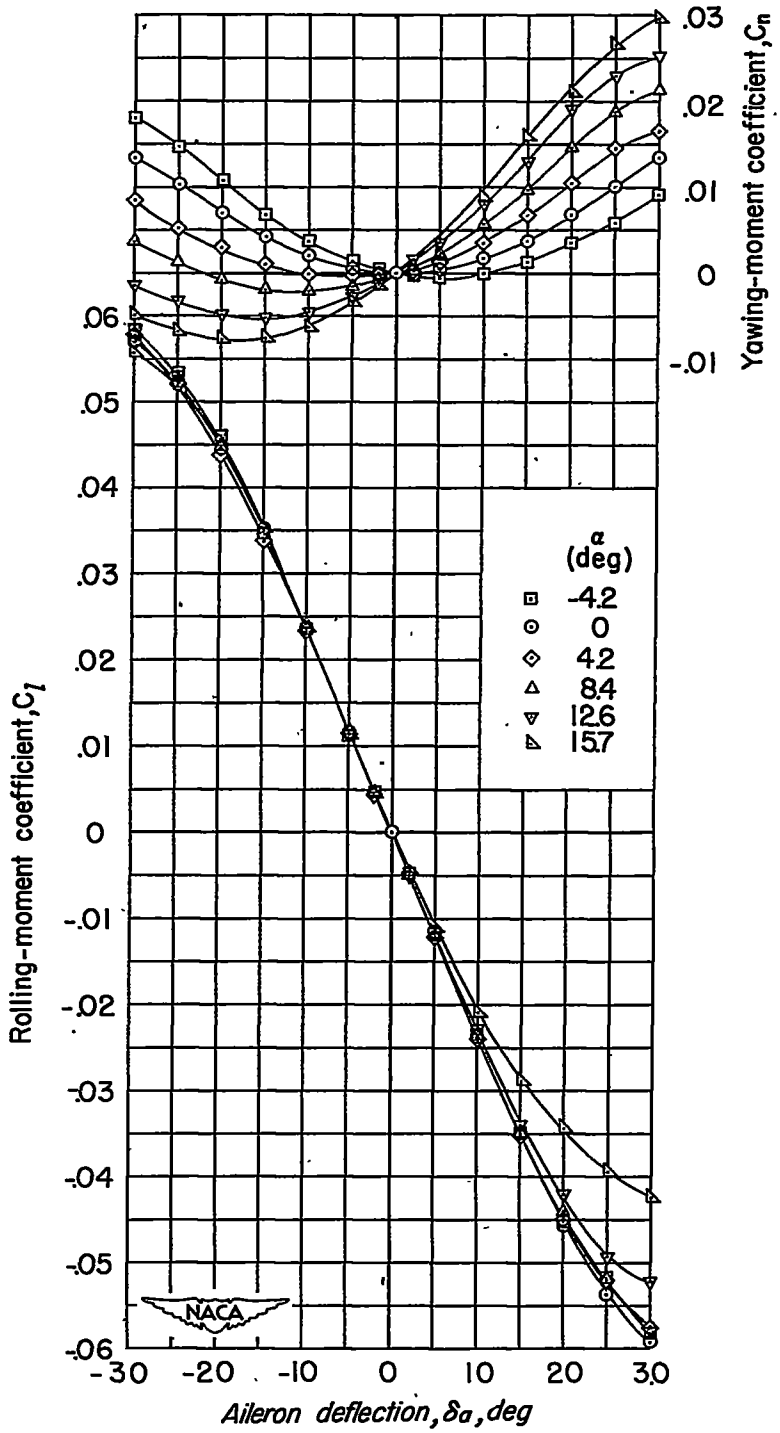

Figure 7.- Variation of lateral control characteristics with aileron deflection on the unswept semispan wing having an aspect ratio of 3.13. $b_a = 0.726\frac{b}{2}$; $y_{a_i} = 0.242\frac{b}{2}$; $y_{a_o} = 0.968\frac{b}{2}$.

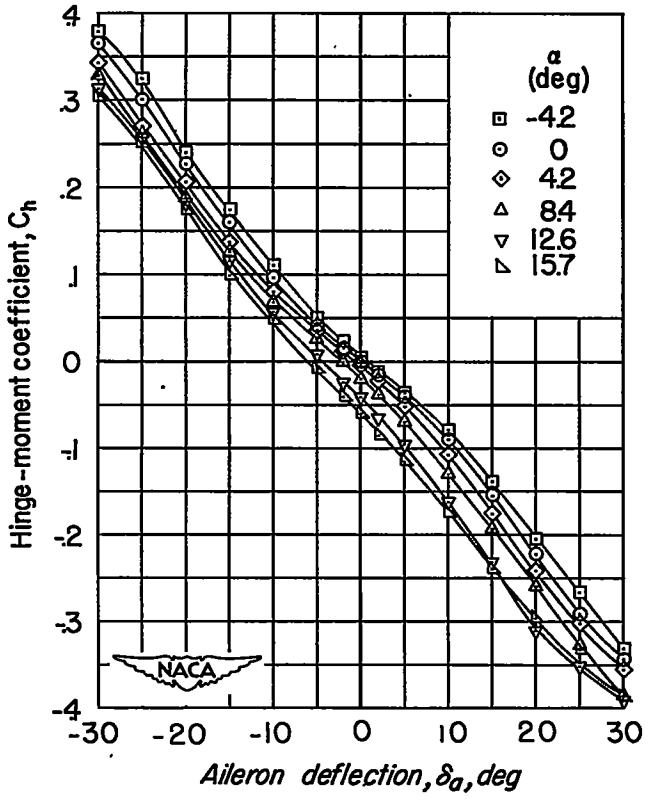

Figure 7.- Concluded.

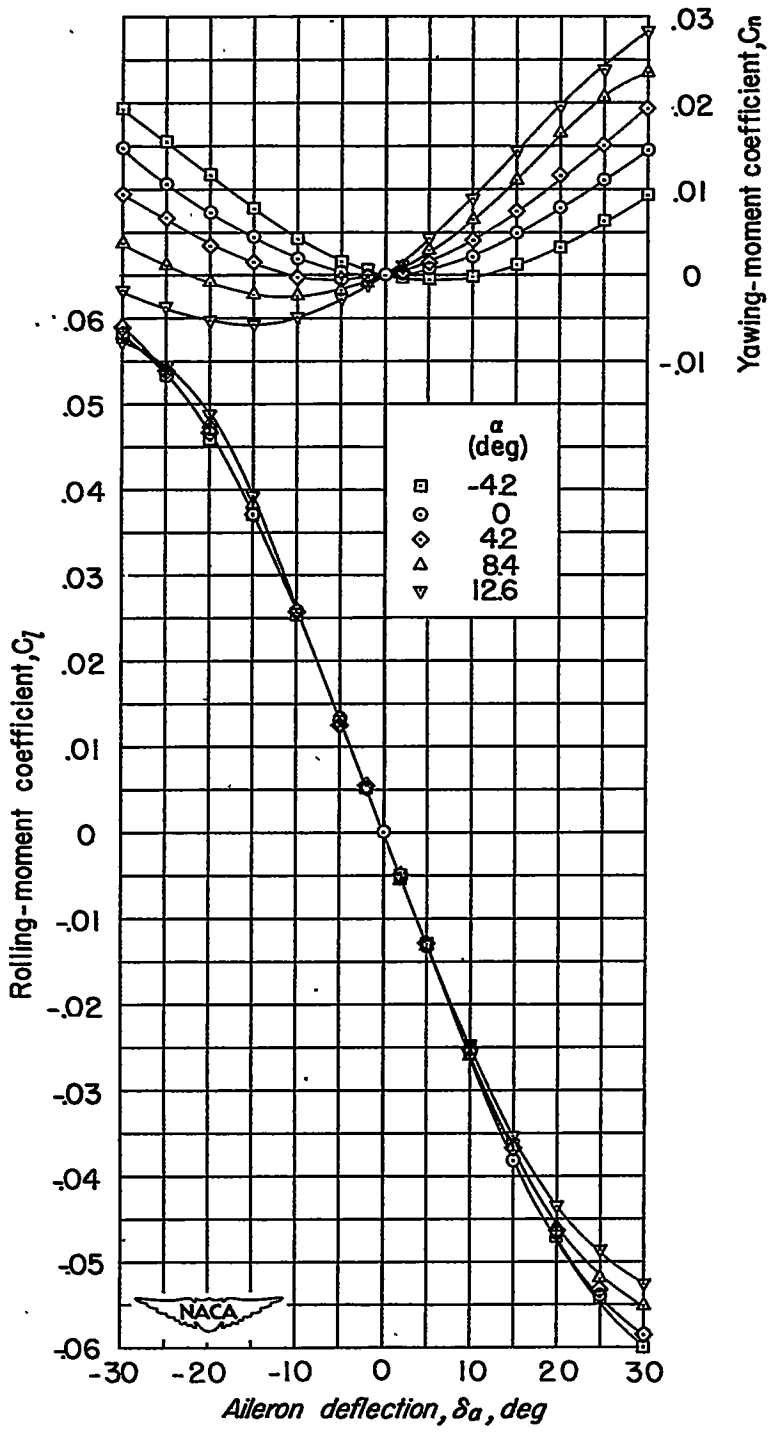

Figure 8.- Variation of lateral control characteristics with aileron deflection on the unswept semispan wing having an aspect ratio of 3.13. $b_a = 0.968\frac{b}{2}$; $y_{a_i} = 0$; $y_{a_o} = 0.968\frac{b}{2}$.

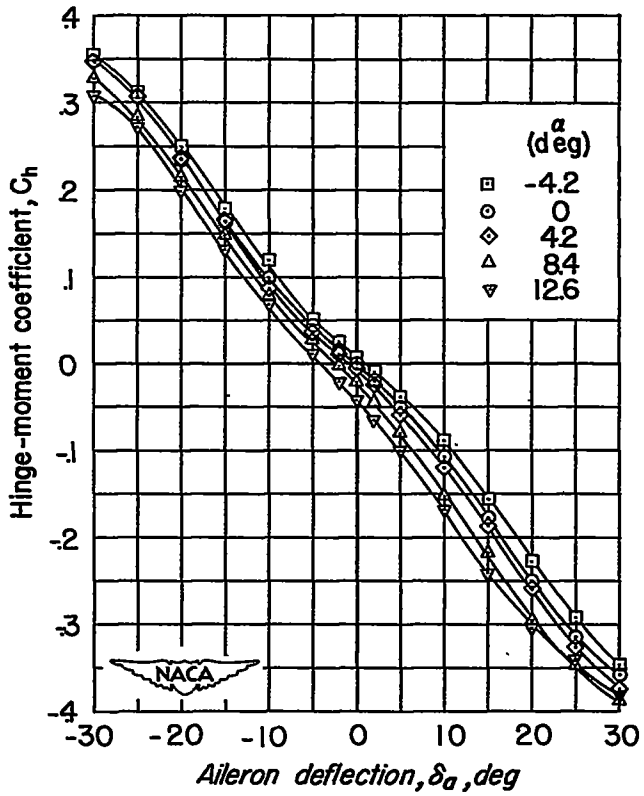

Figure 8.- Concluded.

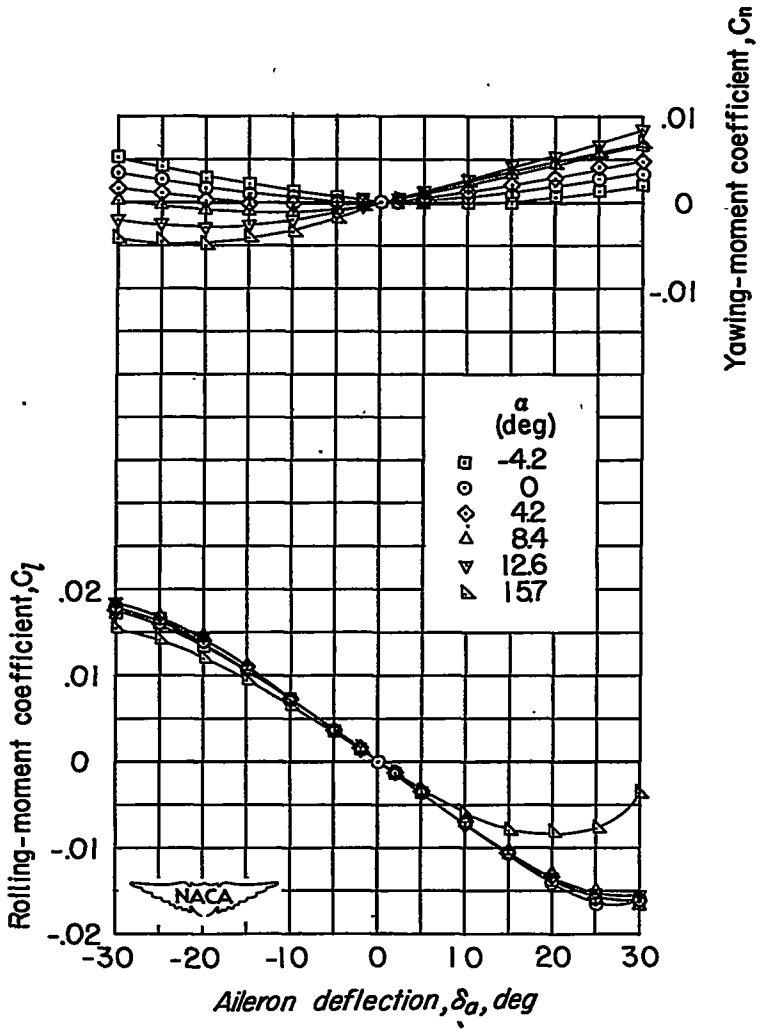

Figure 9.- Variation of lateral control characteristics with aileron deflection on the unswept semispan wing having an aspect ratio of 3.13. $b_a = 0.484\frac{b}{2}$; $y_{a_i} = 0$; $y_{a_o} = 0.484\frac{b}{2}$.

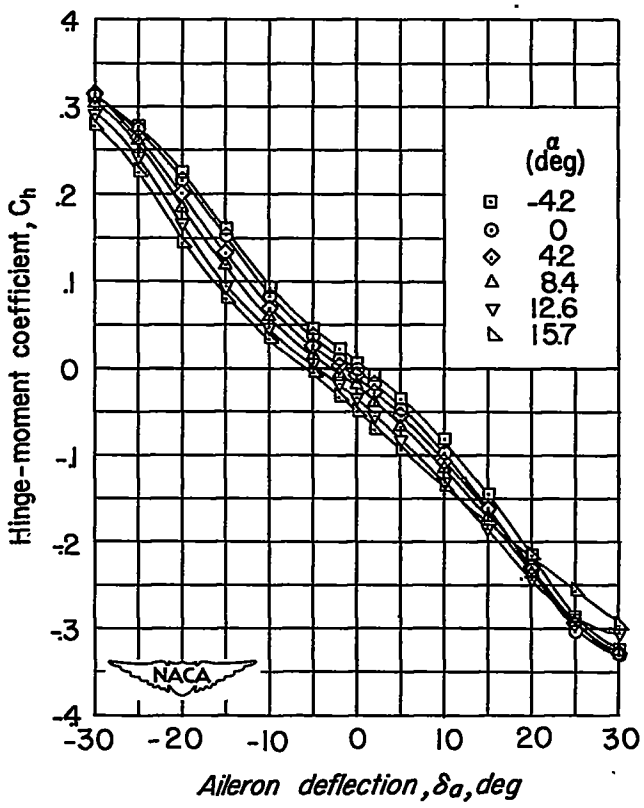

Figure 9.- Concluded.

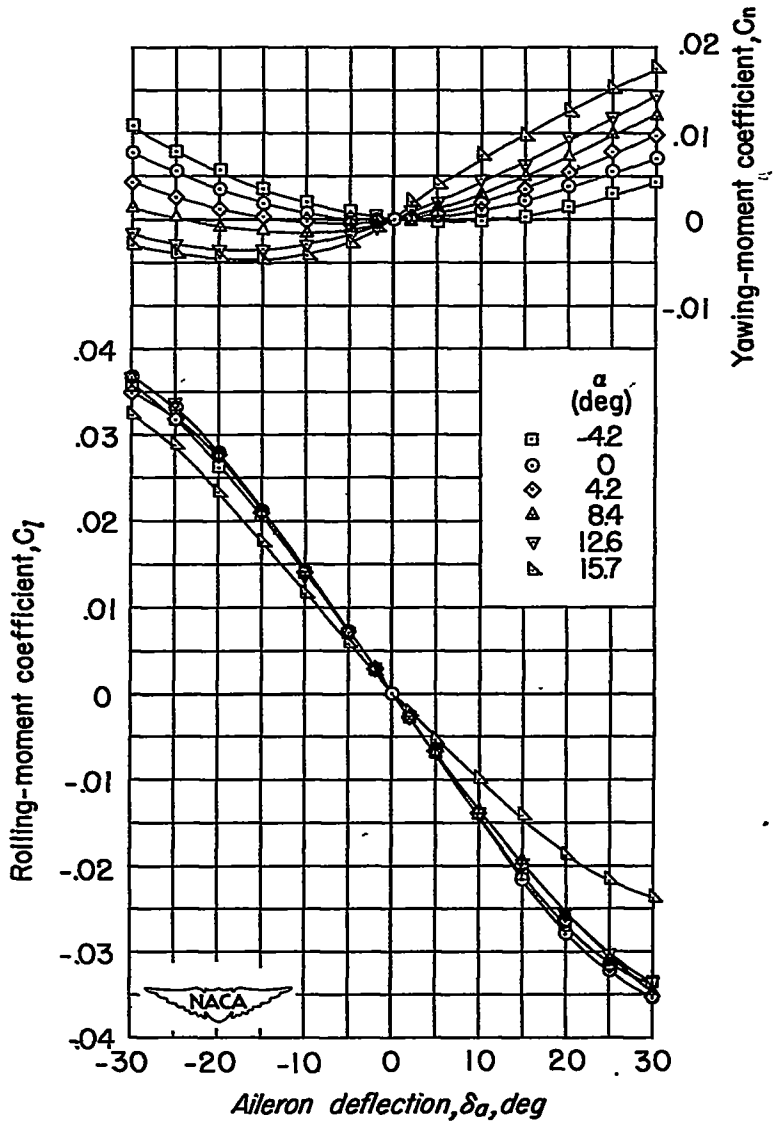

Figure 10.- Variation of lateral control characteristics with aileron deflection on the unswept semispan wing having an aspect ratio of 3.13. $b_a = 0.484\frac{b}{2}$; $y_{a_i} = 0.242\frac{b}{2}$; $y_{a_o} = 0.726\frac{b}{2}$.

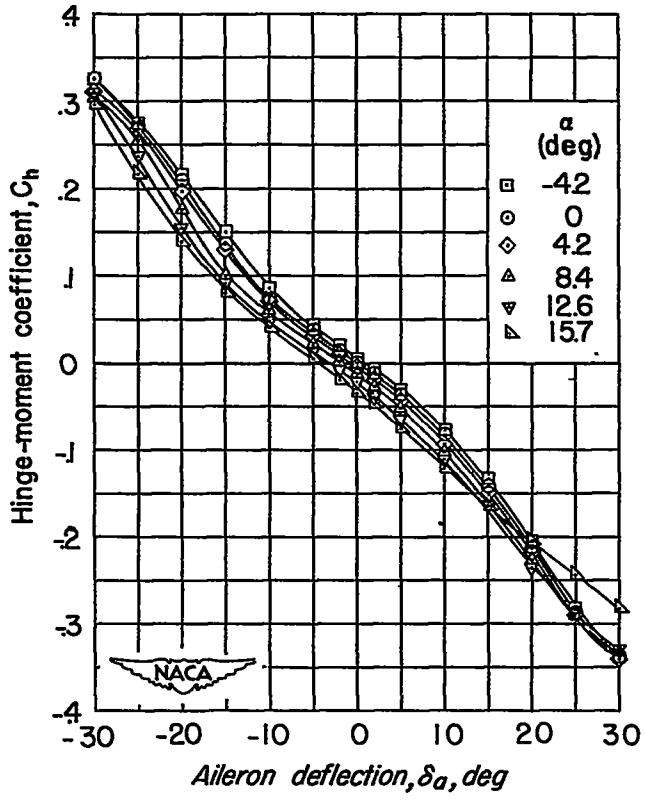

Figure 10.- Concluded.

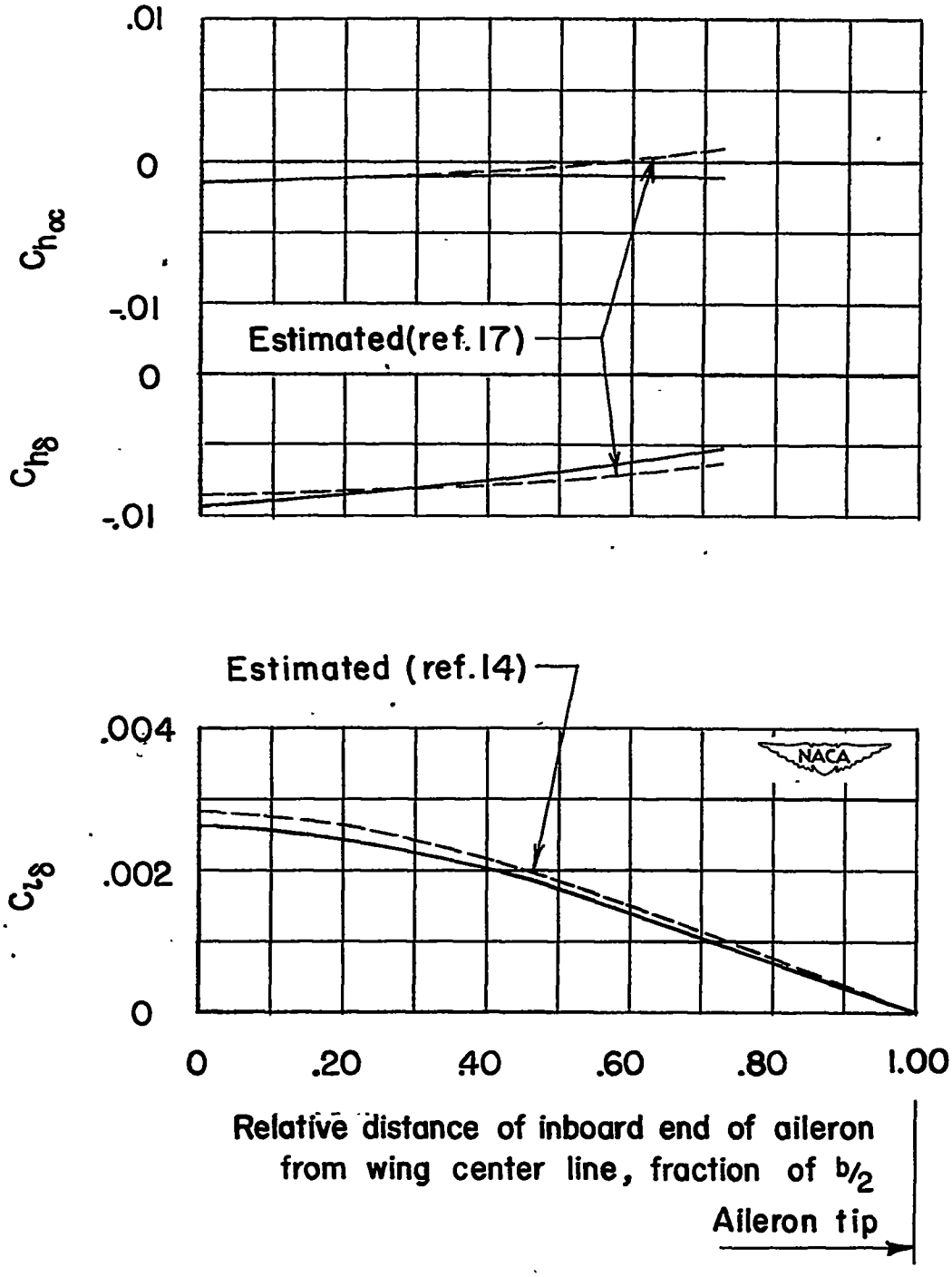

Figure 11.- Variation of aileron parameters C_{l_δ}, C_{h_δ}, and C_{h_α} with relative position of inboard end of aileron on the unswept semispan wing having an aspect ratio of 3.13. $y_{a_o} = 0.968\frac{b}{2}$.